EFDA–JET–CP(10)06/14

F. Koechl, G. Corrigan, D. Frigione, L. Garzotti, G. Kamelander, P.T. Lang,
H. Nehme, V. Parail, B. Pégourié, M. Valovic, S. Wiesen
and JET EFDA contributors

Integrated Modelling of Pellet Experiments at JET

Integrated Modelling of Pellet Experiments at JET

F. Koechl[1], G. Corrigan[2], D. Frigione[3], L. Garzotti[2], G. Kamelander[1], P.T. Lang[4], H. Nehme[5], V. Parail[2], B. Pégourié[5], M. Valovic[2], S. Wiesen[6]
and JET EFDA contributors*

JET-EFDA, Culham Science Centre, OX14 3DB, Abingdon, UK

[1]Association EURATOM-ÖAW/ATI, Atominstitut, TU Wien, 1020 Vienna, Austria
[2]Association EURATOM-CCFE Fusion Association, Culham Science Centre, OX14 3DB, Abingdon, OXON, UK
[3]Association EURATOM-ENEA sulla Fusione, CP 65, Frascati, Rome, Italy
[4]MPI für Plasmaphysik, EURATOM Association, Boltzmannstr. 2, 85748 Garching, Germany
[5]Association EURATOM-CEA, CEA, IRFM, 13108 Saint-Paul-lez-Durance, France
[6]Institut für Energieforschung-Plasmaphysik, FZ Jülich, TEC, Association EURATOM-FZJ, Germany
** See annex of F. Romanelli et al, "Overview of JET Results",*
(Proc. 22 [nd] IAEA Fusion Energy Conference, Geneva, Switzerland (2008)).

Preprint of Paper to be submitted for publication in Proceedings of the
37th EPS Conference on Plasma Physics, Dublin, Ireland.
(21st June 2010 - 25th June 2010)

1. INTRODUCTION

ITER-like plasmas with edge-localised pellet fuelling need to be modelled in an integrated approach combining transport codes for the plasma core and Scrape-Off Layer (SOL) with a pellet code based on first principles assumptions. This would allow to properly account for strong interactions between the pellet injection and particle deposition behaviour and edge and core transport properties, which together determine the fuelling efficiency and affect the overall plasma performance [1]. At JET, first integrated predictive modelling has been performed for recent pellet experiments with the new High Frequency Pellet Injector (HFPI) [2-5]. With the help of synthetic diagnostics, i.e. tools that convert the simulation data into diagnostic measures, it was possible to draw direct comparisons with measurements from new high resolution pellet diagnostic systems available at JET and to compensate for reduced measurement capabilities in conditions with low signal-to-noise ratio, enabling the study of the E×B drift of ablated pellet particles, the pellet retention time, the pellet penetration length required for ELM triggering and the interaction between pellet-triggered ELMs and pellet fuelling.

2. SIMULATION CONDITIONS

The JET Integrated Transport Suite of Codes JINTRAC, which includes the pellet ablation and deposition code HPI2, the 1.5D core transport code JETTO [6] and the multi-fluid SOL code EDGE2D-EIRENE [7,8], has been run to simulate pellet injections in L-mode (Pulse No's: 76411, 76570, 78605, 78606) and H-mode target plasmas (Pulse No's: 77864, 78606) from the Low Field Side (LFS) and the Vertical High Field Side (VHFS) of the JET tokamak. HPI2 determines the pellet particle source by application of a pellet ablation model which is based on the Neutral Gas and Plasmoid Shielding (NGPS) description [9]. Plasmoid drift, the E×B drift of the ionised ablated pellet material cloudlets, can be taken into account following a four-fluids Lagrangian model for the plasmoid homogenisation process [10]. In JETTO, the transport equations are solved for plasma current, temperatures and density. Transport coefficients are calculated according to the mixed Bohm/gyroBohm transport model [11]. Edge Transport Barrier (ETB) zones in H-mode are established by transport reduction to neoclassical level; if the normalised pressure gradient within the ETB exceeds a prescribed value, ELM events are emulated by a temporary sharp increase in edge transport. In the SOL, perpendicular transport is defined by the diffusivities at the separatrix; longitudinal transport follows Braginskii's approximation. Gas puff injection at a low puffing rate up to 10^{21} s^{-1} was considered according to experimental settings. Particles are pumped out at the sub-divertor region with the pump efficiency prescribed by an albedo value. The JINTRAC simulations were iterated in steps of 10-30ms, with the neutral distribution recalculated every 100-300ms. Synthetic measurement data is produced for the JET interferometry, Thomson scattering, Electron Cyclotron Emission (ECE), and D_α emission diagnostic systems.

3. PLASMOID DRIFT

The increase in line-integrated core and edge densities after pellet injection measured by

interferometry has been evaluated to demonstrate the existence of a small plasmoid drift in JET L-mode target plasmas ($n_{e0} \sim 2.5\times10^{19}$ m^{-3}, $T_{e0} \sim 2$keV, $B_0 \sim 2.3$T), and to determine the average drift displacement of the pellet particles. Pellets injected from the LFS would penetrate more deeply into the plasma, because their initial speed (~167m/s versus ~145m/s for VHFS pellets) and their relative velocity compared to the flux surfaces is higher as compared to VHFS pellets. However, due to the outward E×B drift displacement, their ratio between core and edge particle deposition is lower as observed in the experiment (Fig.1). The deposition behaviour can be roughly reproduced by JINTRAC simulations except for massive pellets leading to an increase in plasma particle content by more than 100% ($r_p > 1.5$mm). For small VHFS pellets, the result is not very clear, due to the influence of accompanying pellet fragments which increase the particle accumulation at the edge. According to the simulation results, the average plasmoid drift for fuelling pellets amounts to ~12cm and ~5cm for LFS and VHFS injections respectively (in terms of mid-plane minor radius coordinates), confirming results from a statistical analysis [12]. Expressed in local Cartesian coordinates, the drift displacement for VHFS pellets can exceed that for LFS pellets though by up to ~30%. This discrepancy can be explained by possible influences from the pellet rocket acceleration and pre-cooling effect [13], which can become important for VHFS injections with long ablation times of more than 4ms [14], and the fact that the drift acceleration scales inversely with the local major radius [10]. According to ECE measurements, the propagation velocity of the pellet-induced temperature drop is significantly enhanced compared to the pellet velocity. This disagreement can only be relaxed by assumption of a small plasmoid drift and electron temperature equilibration times that are comparable to the characteristic time for the drift displacement.

4. POST PELLET TRANSPORT

The evolution of the plasma after pellet injection can best be reproduced by JINTRAC, if the particle diffusivity in the region affected by the pellet is increased by a factor of 3–5 compared to the nominal Bohm/gyroBohm level; this is in agreement with previous observations [15]. The evolution of the edge density depends on the SOL conditions. The pump efficiency is increased to account for a higher neutral pressure and strongly enhanced plasma particle transport that appears to scale with the plasma density in the SOL in low pressure conditions [16] rather than with the transport level at the plasma edge. For the same pellet trains analysed in Fig.1, the pellet retention time [17] has been calculated and compared with JINTRAC calculations (Fig.2). As expected, the fuelling efficiency is improved for VHFS injections caused by E×B drift-induced deeper particle deposition.

5. PACING PELLETS

For ELM-pacing sized pellets ($r_p < 1$ mm) injected into L-mode plasmas at a speed of $V_p \sim 130$m/s, the penetration length has been calculated and compared with measurement data to determine the range of effective pellet masses reaching the plasma. A large mass scatter up to a maximum of ~4×10^{19} D has been observed (Fig.4). Assuming pellets covering the same mass range reach ELMy H-mode target plasmas, the minimum required penetration length for ELM triggering could be estimated by

simulations, which seems to be comparable to the width of the ETB zone [2,3] (Fig.5). JINTRAC simulations of pellet-fuelled ELMy H-mode plasmas have shown that the fuelling efficiency can be significantly reduced due to ELM triggering, if the pellet particle deposition takes place mainly in the ETB zone, as it is the case for LFS injections at JET. For ITER, a similar behaviour is expected even for injections from the high field side, if the E¥B drift will be lower than predicted.

CONCLUSIONS

With the help of integrated modelling and the synthetic diagnostics available with JINTRAC, evidence for the existence of an E×B drift displacement has been given for individual pellets. Particle transport seems to be enhanced compared to the level predicted by the mixed Bohm/ gyroBohm model in the plasma edge and the SOL after pellet injection. The pellet penetration length required for ELM triggering in JET has been estimated and the detrimental effect of ELM triggering for edge-localised pellet fuelling has been demonstrated. These results confirm the assumption that the ITER performance targets can only be reached with pellet fuelling from the high field side relying on the E×B drift [18,19].

ACKNOWLEDGEMENTS

This work was supported by EURATOM and carried out within the framework of the European Fusion Development Agreement. The views and opinions expressed herein do not necessarily reflect those of the European Commission.

REFERENCES

[1]. B. Pégourié, Plasma Physics and Controlled Fusion **49** (2007) R87–R160.
[2]. B. Alper et al., Insight from fast data on pellet ELM pacing at JET, P-2.173.
[3]. L. Garzotti et al., Investigating pellet ELM triggering physics using the new small size pellet launcher at JET, P-2.131.
[4]. G. Kocsis et al., Comparison of the onset of pellet triggered and spontaneous ELMs, P-4.136.
[5]. R. Wenninger et al., Filament footprints of pellet induced ELMs observed on divertor target, P-4.173.
[6]. G. Cenacchi, A. Taroni, Rapporto ENEA RT/TIB/88/5 (1988).
[7]. R. Simonini et al., Contribution to Plasma Physics **34** (1994) 368-373.
[8]. D. Reiter, EIRENE Code Manual, www.eirene.de (1992).
[9]. B. Pégourié et al., Plasma Physics and Controlled Fusion **47** (2005) 17-35.
[10]. B. Pégourié et al., Nuclear Fusion **47** (2007) 44-56.
[11]. M. Erba et al., Plasma Physics and Controlled Fusion **39** (1997) 261-276.
[12]. F. Koechl et al., Proc. 34th EPS Conf. on Plasma Physics (Warsaw, Poland) 31F P-1.143.
[13]. H.W. Müller et al., Phys. Rev. Lett. **83** (1999) 2199-2202.
[14]. G. Kamelander et al., Proceedings 35th EPS Conference on Plasma Physics (Hersonissos, Crete, Greece) **32D** P-4.104.

[15]. L. Garzotti et al., Proc. 27th EPS Conference on Controlled Fusion and Plasma Physics (Budapest, Hungary) **24**B 316-319.
[16]. J. P. Graves et al., Plasma Physics and Controlled Fusion **47** (2005) L1–L9.
[17]. M. Valovic et al., Nuclear Fusion **48** (2008) 075006.
[18]. V. Parail et al., Nuclear Fusion **49** (2009) 075030.
[19]. B. Pégourié et al., Plasma Phys. Control. Fusion **51** (2009) 124023.

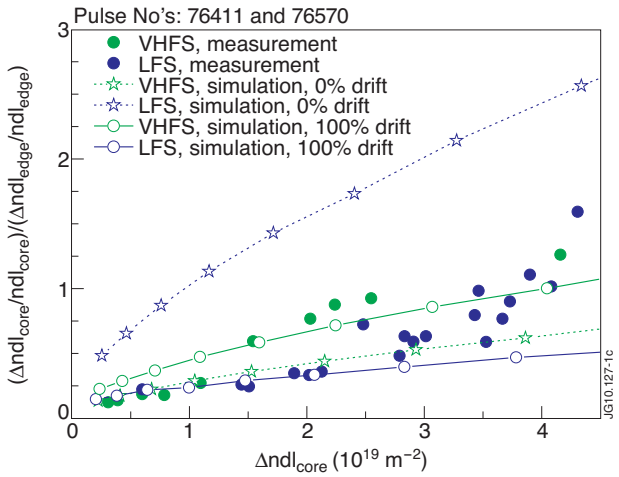

Figure 1: Ratio between the relative increase of line-integrated plasma core and edge densities measured along the JET interferometry lines of sight in dependence of the increase in line-integrated core density after pellet injection.

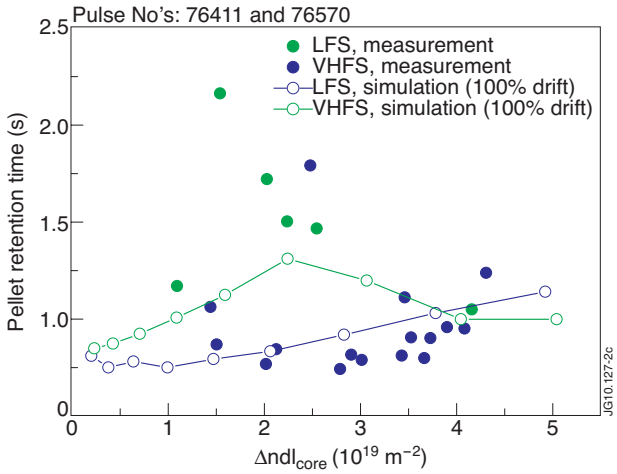

Figure 2: Pellet particle retention time measured as exponential decay time of the line-integrated plasma core density signal after pellet injection in dependence of the pellet-caused increase in line-integrated core density.

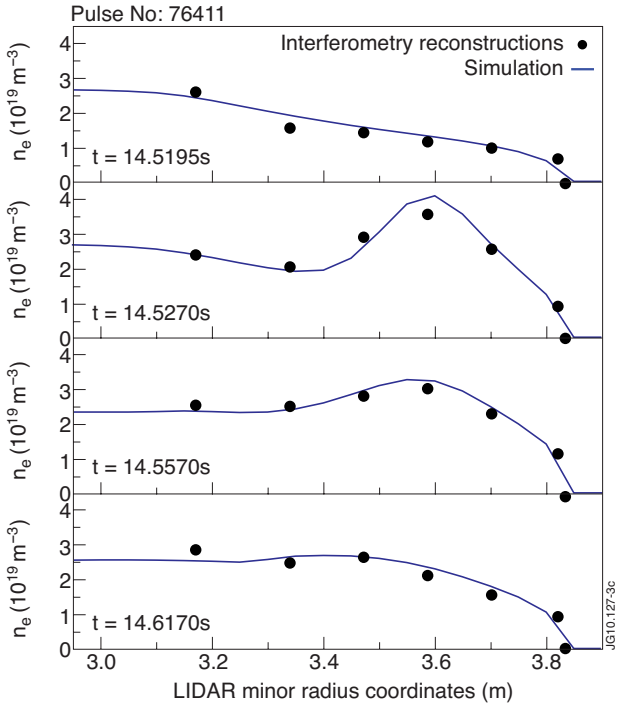

Figure 3: Simulated density evolution for a pellet (r_p = 1.6mm, V_p = 160m/s) injected from the LFS into a JET L-mode target plasma assuming increased edge particle transport (5x compared to Bohm/gyroBohm level) after injection; the data is compared with profile reconstructions from interferometry data.

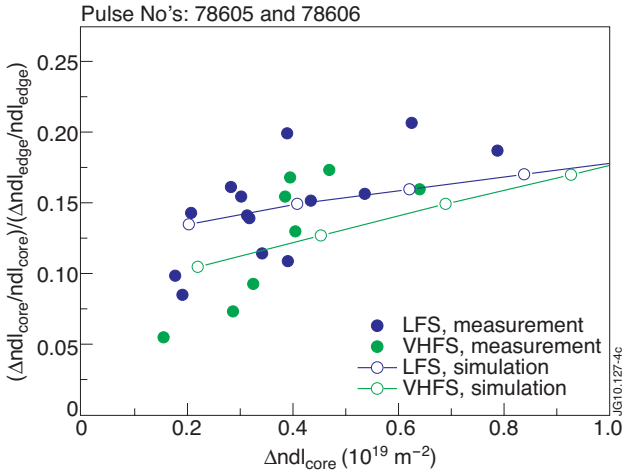

Figure 4: Ratio between the relative increase of line-integrated plasma core and edge densities measured along the JET interferometry lines of sight in dependence of the increase in line-integrated core density after pellet injection, for small pellets used for ELM triggering. According to the simulation results, the upper mass limit is ~4×10^{19} D.

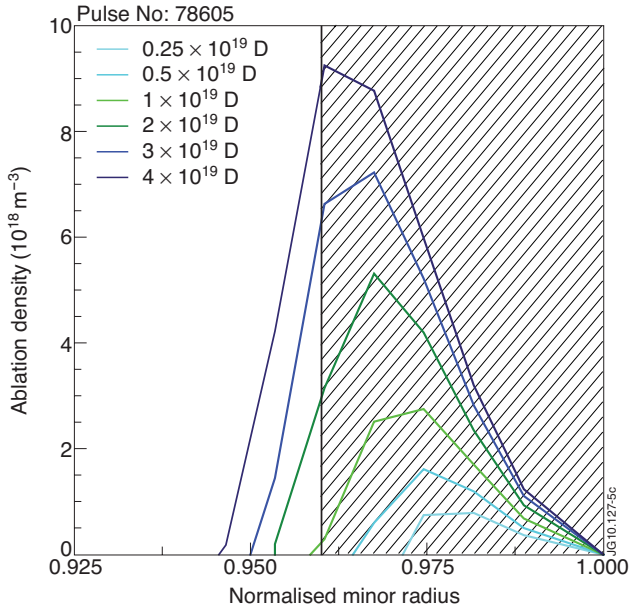

Figure 5: Pellet ablation profiles for small pellets injected from the LFS into a JET H-mode plasma; pellets with a mass of > 10^{19} D seem to reliably trigger ELMs [2]. The shaded area indicates the ETB zone.